PERGAMON

Deep-Sea Research I 49 (2002) 321–338

DEEP-SEA RESEARCH
PART I

www.elsevier.com/locate/dsr

The annual cycle and biological effects of the Costa Rica Dome

Paul C. Fiedler*

NOAA/National Marine Fisheries Service (NMFS), Southwest Fisheries Science Center, P.O. Box 271, La Jolla, CA 92038, USA

Received 20 October 2000; received in revised form 17 May 2001; accepted 4 September 2001

Abstract

The Costa Rica Dome is similar to other tropical thermocline domes in several respects: it is part of an east–west thermocline ridge associated with the equatorial circulation, surface currents flow cyclonically around it, and its seasonal evolution is affected by large-scale wind patterns. The Costa Rica Dome is unique because it is also forced by a coastal wind jet. Monthly climatological fields of thermocline depth and physical forcing variables (wind stress curl and surface current divergence) were analyzed to examine the structure and seasonal evolution of the dome. The annual cycle of the dome can be explained by wind forcing in four stages: (1) *coastal shoaling* of the thermocline off the Gulf of Papagayo during February–April, forced by Ekman pumping on the equatorward side of the Papagayo wind jet; (2) *separation from the coast* during May–June when the intertropical convergence zone (ITCZ) moves north to the countercurrent thermocline ridge, the wind jet stops, and the North Equatorial Countercurrent extends toward the coast on the equatorward flank of the ridge; (3) *countercurrent thermocline ridging* during July–November, when the dome expands to the west as the countercurrent thermocline ridge shoals beneath a band of cyclonic wind stress curl on the poleward side of the ITCZ; and (4) *deepening* during December–January when the ITCZ moves south and strong trade winds blow over the dome. Coastal eddies may be involved in the coastal shoaling observed during February–March. A seasonally predictable, strong, and shallow thermocline makes the Costa Rica Dome a distinct biological habitat where phytoplankton and zooplankton biomass are higher than in surrounding tropical waters. The physical structure and biological productivity of the dome affect the distribution and feeding of whales and dolphins, probably through forage availability. Published by Elsevier Science Ltd.

Keywords: Equatorial circulation; Trade winds; Ekman pumping; Thermocline; Biological production; Annual variations

1. Introduction

The Costa Rica Dome, located off the coast of Central America, is a shoaling of the generally strong (large dT/dz) and shallow thermocline of the eastern tropical Pacific Ocean. It was first observed in 1948 (Wyrtki, 1964) and first described by Cromwell (1958). The dome has been observed and studied several times since the late 1950s, when a productive tuna fishery began to develop in the region. However, it has been sampled intensively, only a few times: the Costa Rica Dome Expedition by the Scripps Tuna Oceanography Research program in 1959 and the Mexican DOMO surveys in 1979–1982 were exceptional for applying much sampling effort in repeated surveys of the dome.

*Fax: +1-858-546-7198.
E-mail address: pfiedler@ucsd.edu (P.C. Fiedler).

0967-0637/02/$ - see front matter Published by Elsevier Science Ltd.
PII: S0967-0637(01)00057-7

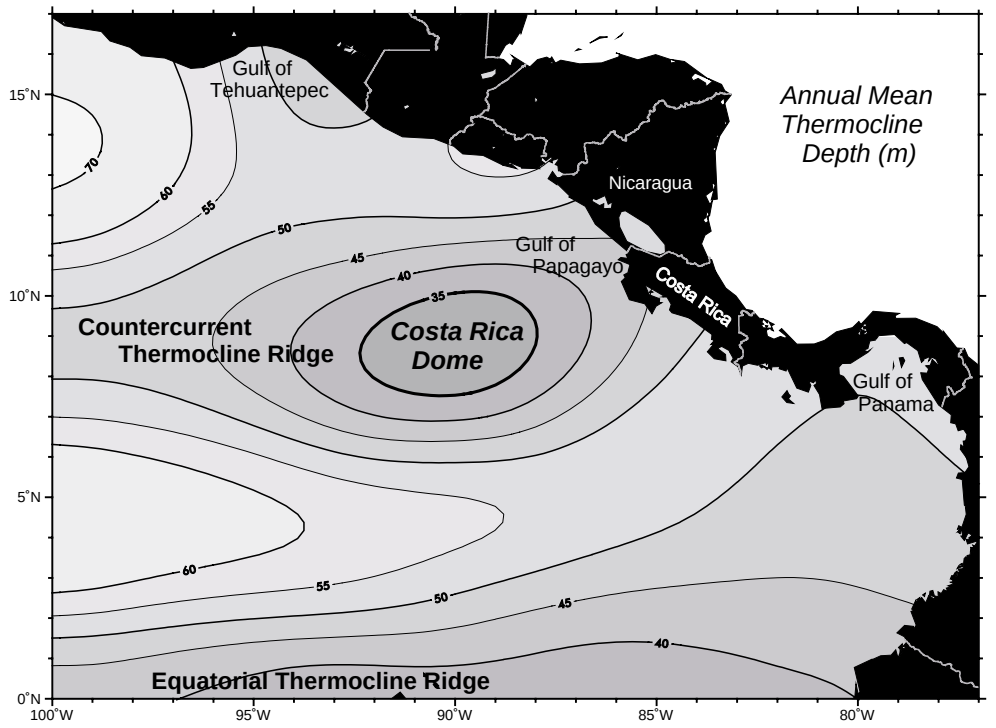

Fig. 1. Annual mean thermocline depth (20°C isotherm depth) in the region of the Costa Rica Dome. Data from World Ocean Database 1998 (Conkright et al., 1999).

The mean position of the dome is near 9°N 90°W, at the end of a thermocline ridge which shoals from west to east across the Pacific, between the westward North Equatorial Current (NEC) and the Eastward North Equatorial Countercurrent (NECC) (Fig. 1). This ridge and the dome extend below the thermocline, to a depth of more than 300 m (Fig. 2). Tropical thermal domes also exist in the eastern Atlantic (the Guinea Dome to the north of the equator and the Angola Dome to the south; Mazeika, 1967) and the western Pacific (Mindanao Dome; Wyrtki, 1961). There is a subthermocline Peru Dome in the southeastern tropical Pacific (Voituriez, 1981).

The Costa Rica Dome is the peak at the terminus of the countercurrent thermocline ridge. The top of the thermocline is about 15 m deep at the dome, compared to 30–40 m to the north and south (Fig. 2, top). The thermocline ridge shoals gradually from west to east, then drops off sharply between the dome and the coast (Fig. 2, bottom). Thus, the dome is a minimum in the annual mean field of thermocline depth, 300–500 km in diameter and centered 300 km off the Gulf of Papagayo between Costa Rica and Nicaragua (Fig. 1).

Surface winds and currents in the region of the Costa Rica Dome change seasonally as the intertropical convergence zone (ITCZ) between the trade wind belts moves north and south with the sun (Fig. 3). The relative strengths of the northeast and southeast trade winds in the region vary considerably during the year. Winter high-pressure systems over the Gulf of Mexico and Caribbean Sea force strong winds through low altitude passes in the mountainous backbone of southern Mexico and Central America. Intense and narrow wind jets blow offshore at the Gulfs of Tehuantepec, Papagayo, and Panama (McCreary et al., 1989; Chelton et al., 2000a, b). In summer, the southeast trade winds blow strongly across the equator as far as 8°N.

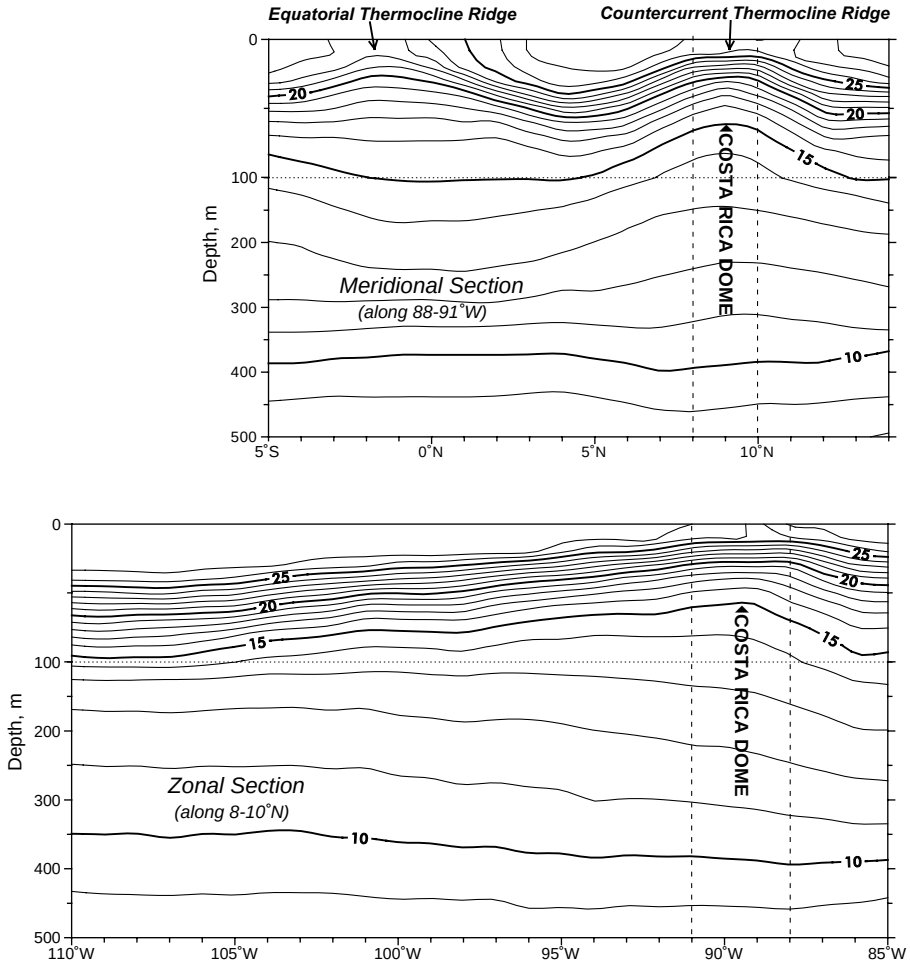

Fig. 2. Annual mean meridional (top) and zonal (bottom) temperature sections through the Costa Rica Dome. Data from World Ocean Database 1998 (Conkright et al., 1999).

The westward NEC and eastward NECC flow in geostrophic balance along the poleward and equatorward slopes, respectively, of the countercurrent thermocline ridge. The westward South Equatorial Current (SEC) flows along the equatorial thermocline ridge. Part of the NECC is deflected north at the coast of Central America and joins the Costa Rica Coastal Current (CRCC), which flows into the NEC. This pattern of cyclonic flow exists only in summer-fall, when it flows around the Costa Rica Dome. The NECC does not extend east of 100°W during February–April.

Cromwell (1958) published the first description of the "Costa Rican Thermal Dome" and noted its relationship to "cyclonic current shear". Wyrtki (1964) elaborated Cromwell's observations using data collected by the Scripps Tuna Oceanography Research program in the late 1950s. He proposed that the steady-state heat balance of thermocline doming was maintained by upwelling "caused by the cyclonic flow around the dome". Upwelling was explained as the result of an adjustment of the geostrophic balance of the NECC as it turned northward at the coast, around the eastern end of the countercurrent thermocline ridge. Although he

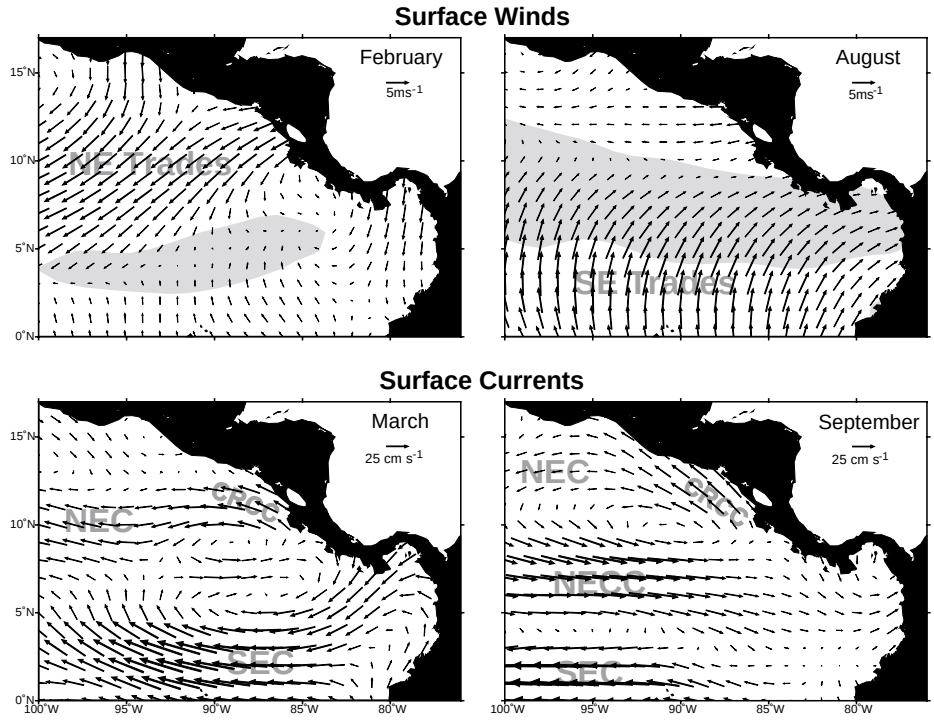

Fig. 3. Mean monthly fields of surface wind velocity (top) and surface current velocity (bottom), representing seasonal extremes in the region of the Costa Rica Dome. Surface winds from COADS (Roy and Mendelssohn, 1995), surface currents from windage-corrected ship drift (NOAA/NODC Ocean Current Drifter Data). Shading indicates surface wind divergence $< -0.5 \times 10^{-7}\,s^{-1}$ (intertopical convergence zone). NEC = North Equatorial Current, SEC = South Equatorial Current, NECC = North Equatorial Countercurrent, CRCC = Costa Rica Coastal Current.

had observations only for May–December, Wyrtki predicted that doming would be weak in early spring when the NECC was weak.

Wyrtki (1964) explicitly dismissed consideration of "an effect of the local wind on the circulation and the upwelling in the dome". In contrast, Hofmann et al. (1981) proposed that upwelling in the dome is forced by Ekman pumping beneath a local, seasonal (May–October) maximum in cyclonic wind stress curl associated with the seasonal northward migration of the ITCZ. Umatani and Yamagata (1991) considered remote wind effects on the Costa Rica Dome. Based on the results of experiments with a high-resolution regional ocean circulation model, they concluded that the dome is eroded by anticyclonic eddies generated on the poleward side of the strong winter wind jet blowing across the Nicaraguan lake district just north of the Gulf of Papagayo in November–March. Note that this wind jet, as well as the resulting eddies, are conventionally labeled "Papagayo" although the core of the jet is about 70 km north of the Gulf of Papagayo (Fig. 3; Chelton et al., 2000b). Regeneration of the model dome during February–April requires vorticity input by a weaker cyclonic eddy formed on the other side of the wind jet. Additional model experiments showed that weak positive local wind stress curl contributes to doming at the eastern end of the countercurrent thermocline ridge during the summer. However, these summer winds alone are not sufficient to generate the dome.

Like the Costa Rica Dome, all tropical thermal domes are associated with a cyclonic turning of predominantly zonal tropical surface currents, as expected in geostrophic balance. The possible

influence of winter coastal eddies is unique to the Costa Rica Dome (Umatani and Yamagata, 1991). Voituriez (1981) proposed that subthermocline doming was the result of subsurface cyclonic flow, however the doming of isotherms below the thermocline dome known as the Costa Rica Dome is not considered here.

This paper will examine monthly climatological fields of thermocline depth and physical variables (wind stress curl and surface current divergence) that might be related to the annual cycle or seasonal evolution of the Costa Rica Dome. Comparison with studies of other tropical thermal domes, in particular, the Guinea and Mindanao Domes which are also located in northern equatorial current systems and are arguably the closest analogs to the Costa Rica Dome, provides some insight. Finally, biological effects of the dome on phytoplankton production and the distribution of zooplankton and other animals are briefly reviewed.

2. Methods

Hydrographic variables were derived from MBT, XBT, and CTD profiles in the NOAA/National Oceanographic Data Center World Ocean Database 1998 CD-ROM Data Set Version 2.0 (Conkright et al., 1999), incorporating the corrections available on-line as of July 20, 2001. A total of 30,030 hydrographic profiles were available in the study area from 1941 to 1996, with 93% from the period 1955–1996. Thermocline depth was defined as the depth of the 20°C isotherm, which is often used as an index of thermocline depth in the tropical ocean (Kessler, 1990). Monthly thermocline depth observations ranged from 1582 in July to 3656 in November (Fig. 4).

Surface current velocities were derived from ship drift data, because available CTD data are not adequate to resolve monthly patterns of geopotential anomaly and geostrophic currents. A total of 130,576 ship drift observations were available in the study area from 1901 to 1987, with 80% from the period 1922 to 1941. Monthly ship drift observations ranged from 5457 in July to 20,793 in March (Fig. 4). Although ship drift is not an ideal estimator of surface currents, Arnault (1987) found that surface currents estimated from ship drift in the tropical Atlantic were nearly equal to the sum of geostophic currents and Ekman drift. Surface current velocities derived from ship drift (NOAA/NODC Ocean Current Drifter Data, CD-ROM NODC-53) were corrected for windage by the method of Richardson (1997).

Wind velocities were extracted from the Comprehensive Ocean Atmosphere Data Set in the "COADS on CD-ROM" data product (Roy and Mendelssohn, 1995). A total of 984,602 wind observations were available in the study area from 1857 to 1990, with 80% from the period 1954 to 1990. Monthly wind observations ranged from 76,372 in December to 88,534 in May (Fig. 4).

Data were gridded with the objective analysis algorithm used to produce the World Ocean Atlas (da Silva et al., 1994), with some modifications for this study area: (1) The radii of influence used in the global analysis were reduced to resolve smaller scale features. (2) The radii of influence were

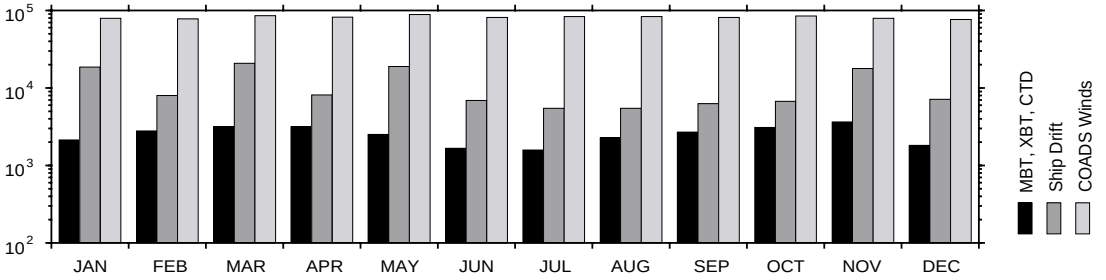

Fig. 4. Monthly totals of temperature profile (MBT, XBT and CTD), ship drift, and COADS wind observations in the Costa Rica Dome study area, 0–17°N, 100–77°W.

anisotropic (meridional/zonal ratio of 0.6, based on variogram analysis of the hydrographic data). Five passes of the objective analysis scheme were performed at scales of 17.5° (10.5°), 13.7° (8.2°), 10.0° (6.0°), 6.2° (3.8°), and 5.0° (3.0°) longitude (latitude). A third modification was made for this study area, in which interannual variability can be as great as variability between months. (3) Raw data were averaged by month–year before being averaged by month, to minimize bias that might arise at a grid point if many observations were made in one or more anomalous years.

Sources of error in 1° monthly fields derived from objective analysis of ship observations are discussed in da Silva et al. (1994). Sampling error for climatological monthly means of temperature and wind speed in the eastern tropical Pacific, due to the concentration of ship observations along well-traveled shipping lanes, should be much less than the root-mean-square errors of ~ 0.3°C and $\sim 0.5\,\mathrm{m\,s^{-1}}$ estimated for individual monthly means in the tropics (da Silva et al., 1994). No wind speed corrections for Beaufort scale estimates, anemometer height, or stability were attempted, assuming that these errors are noise that will not substantially affect the climatological wind stress fields analyzed here.

Wind velocity was converted to wind stress ($\mathrm{N\,m^{-2}}$) using an air density of $1.2\,\mathrm{kg\,m^{-3}}$ and a drag coefficient equal to 1.2×10^{-3} for wind speeds $< 11\,\mathrm{m\,s^{-1}}$ and increasing by 0.065×10^{-3} $(\mathrm{m\,s^{-1}})^{-1}$ for stronger winds (Large and Pond, 1981). For calculation of both wind stress curl $(= \mathrm{d}v/\mathrm{d}x - \mathrm{d}u/\mathrm{d}y)$ and surface current divergence $(= \mathrm{d}u/\mathrm{d}x + \mathrm{d}v/\mathrm{d}y$, where u is eastward and v is northward wind stress or surface current), u and v were gridded at 0.5° resolution. The derivatives were then approximated as linear regressions through grid values within ± 1.5° latitude or longitude from each grid point. For surface current divergence, flow was set to zero at the coast.

Biological data were obtained from several sources. Monthly mean SeaWiFS (Sea-viewing Wide Field-of-view Sensor, http://seawifs.gsfc.nasa.gov/SEAWIFS.html) chlorophyll fields were calculated from Level 3 monthly standard mapped image products (chlorophyll a concentration, October 1997–July 2001, 9-km resolution at the equator, version 3 reprocessing). The SeaWiFS data cover one extreme El Niño year and two moderate La Niña years: while the monthly climatologies may change somewhat as the data set is extended, they are the best available at this time. The spatial and temporal coverage of the 3- to 4-yr SeaWiFS chlorophyll climatologies are considerably more complete than the 8- to 9-yr CZCS climatologies (1978–1986). Historical zooplankton volume and nitrate data were obtained from NOAA/National Oceanographic Data Center. The sample coverage of these data sets were not sufficient for monthly analysis, so only mean fields are presented.

3. Results

The annual cycle of the Costa Rica Dome is illustrated by maps of monthly mean thermocline depth (Fig. 5). In January, the dome is far offshore (92°W) and relatively deep; thermocline depth is > 33 m. In February, the thermocline begins to shoal at the coast on the equatorward side of the Gulf of Papagayo. Coastal shoaling increases during March and April. The elevation of the thermocline begins to look like a dome in April, but remains connected to the coast. During May and June, the dome separates from the coast. The dome deepens somewhat during June, but by July, it is a distinct offshore dome. From July through October, the dome increases in size, primarily to the west along the countercurrent thermocline ridge. The dome remains shallow and extends slightly northward towards the Gulf of Tehuantepec in November, then decreases in size as the countercurrent thermocline ridge deepens in December. Thus, the annual cycle of the dome consists of: (1) *coastal shoaling* in February–April, (2) *separation from the coast* in May–June, (3) *countercurrent thermocline ridging* in July–November, and (4) *deepening* in December–January.

Annual cycles of winds and wind stress curl (Fig. 6) and ship drift surface currents and surface current divergence (Fig. 7) are presented along with the cycle of doming (35 m thermocline depth contour) to examine interrelationships. The annual

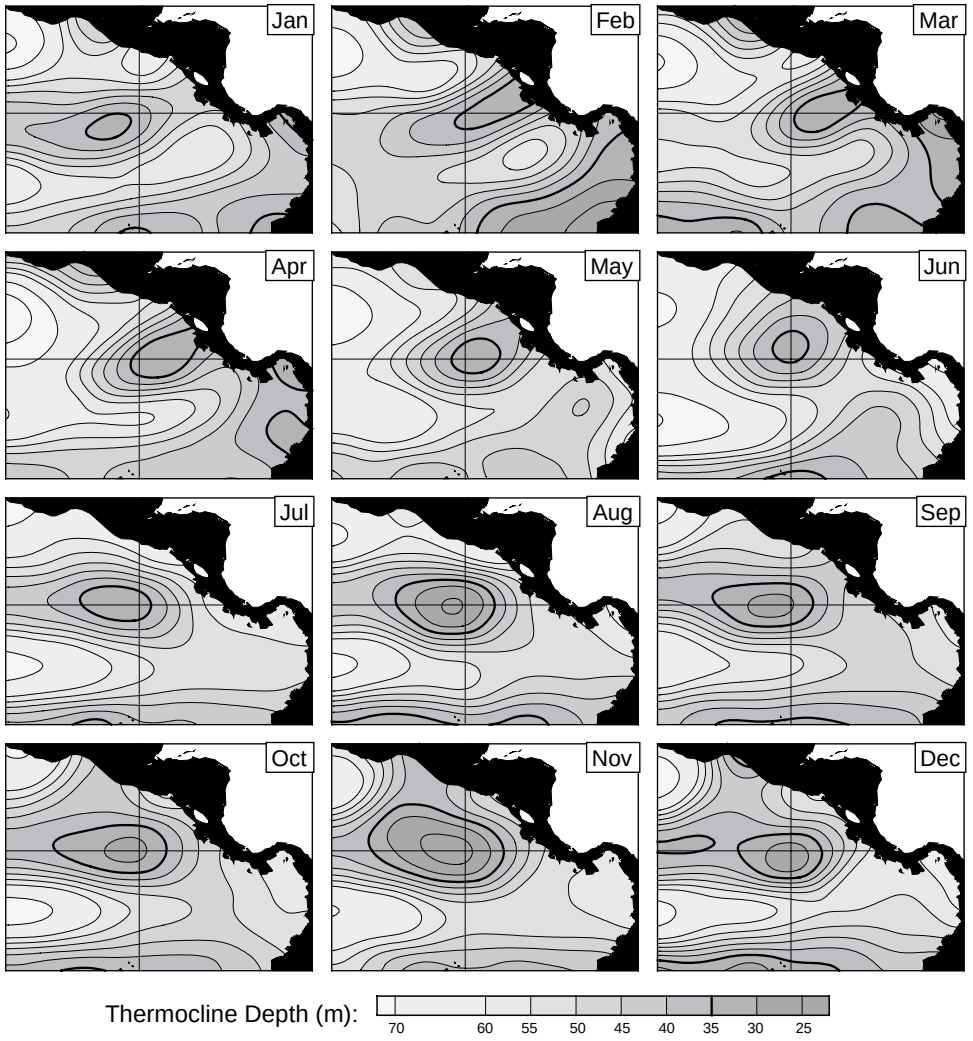

Fig. 5. Monthly mean fields of thermocline depth (20°C isotherm depth) in the region of the Costa Rica Dome. Grid lines are at 9°N and 90°W. Data from World Ocean Database 1998 (Conkright et al., 1999).

cycle of doming and concurrent physical forcing variables can be summarized as follows.

In January, the countercurrent thermocline ridge is relatively deep. A weak doming at about 8°N, 92°W (Fig. 5) is a remnant of the preceding year's Costa Rica Dome. The Papagayo wind jet has been blowing strongly to the WSW since December (Fig. 6). The wind jet produces two lobes of wind stress curl extending off the coast: a negative (anticyclonic) lobe on the poleward side of the jet and a stronger positive (cyclonic) lobe on the equatorward side of the jet. The same pattern of wind stress curl is produced by the Tehuantepec wind jet, which begins blowing strongly in November. An important difference between the Tehuantepec and Papagayo wind stress curl patterns is that the lobe of cyclonic curl on the equatorward side of the Papagayo jet is contiguous with the band of cyclonic curl on the northern side of the ITCZ.

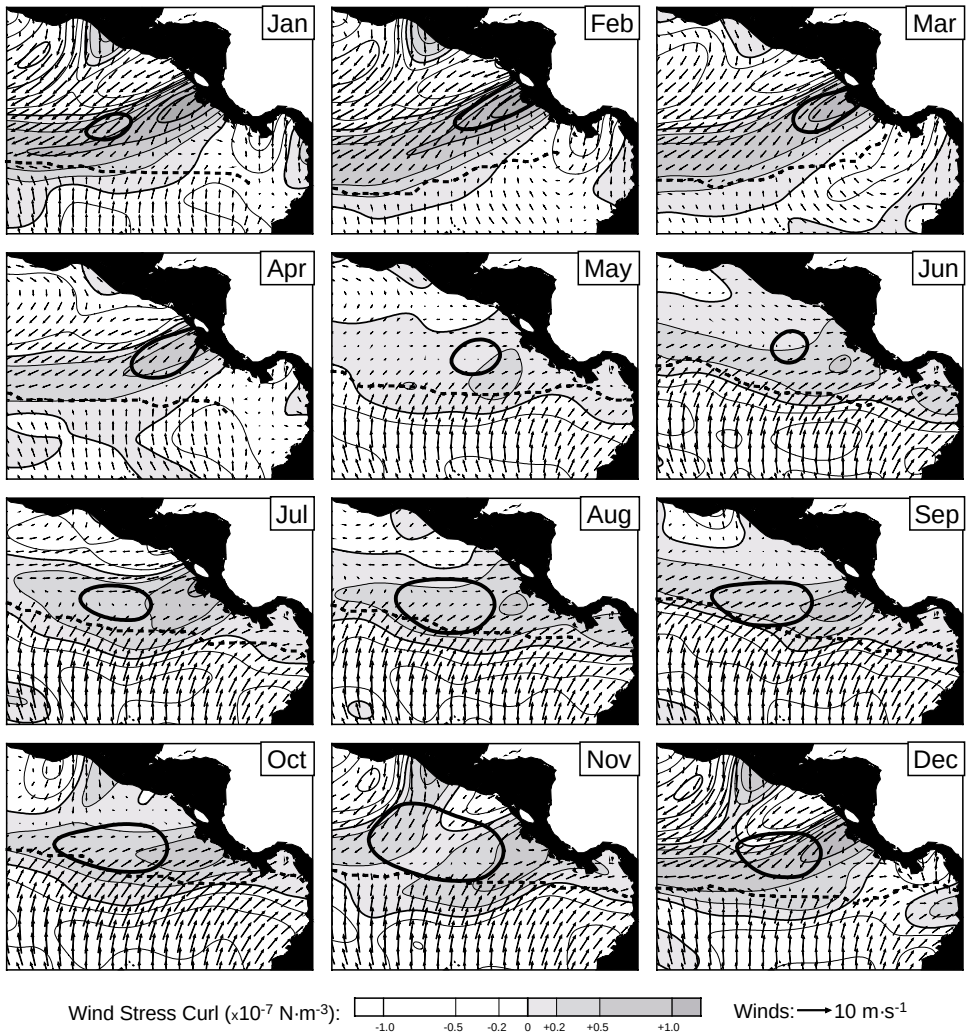

Fig. 6. Monthly mean fields of winds and wind stress curl in the region of the Costa Rica Dome. Dashed line marks the meridional minimum in surface wind divergence (ITCZ). Monthly positions of the Costa Rica Dome (35 m thermocline depth contour, thick lines) from Fig. 5. Data from COADS (Roy and Mendelssohn, 1995).

From February through April, thermocline shoaling occurs at the coast directly beneath the cyclonic wind stress curl associated with the Papagayo wind jet. Strong surface current divergence is evident in the ship drift data at this location (Fig. 7). The ITCZ is at its annual southernmost extreme in February. As coastal shoaling continues during March and April, the ITCZ moves to the north with two important results: (1) the Papagayo wind jet weakens, and (2) the zonal band of cyclonic curl on the northern side of the ITCZ moves north to a location over the countercurrent thermocline ridge. The thermocline ridge deepens to the west of 90°W, however, as it shoals near the coast at this time (Fig. 5).

The dome begins to separate from the coast in May, when the Papagayo wind jet stops and the associated cyclonic curl and surface current divergence weaken. At the same time, the SE trade

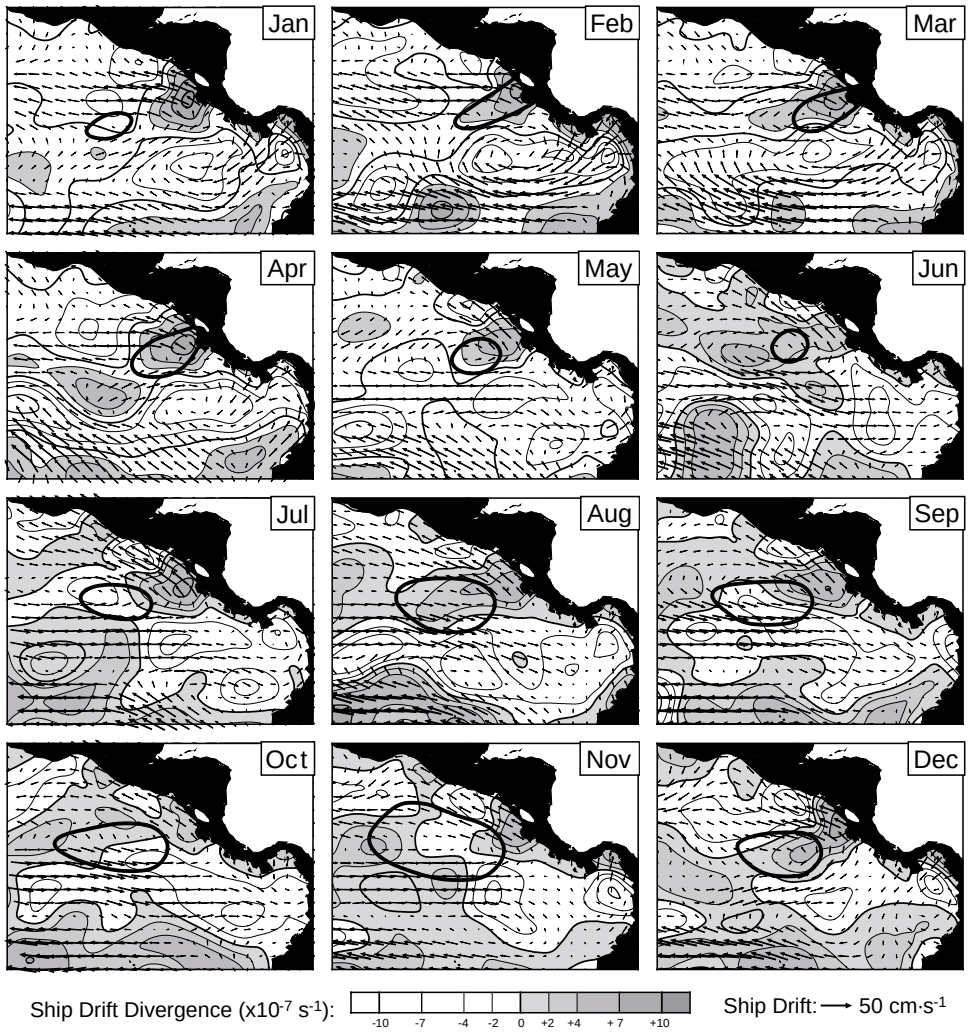

Fig. 7. Monthly mean fields of ship drift surface currents and surface current divergence in the region of the Costa Rica Dome. Monthly positions of the Costa Rica Dome (35 m thermocline depth contour, thick lines) from Fig. 5. Data from NOAA/NODC Ocean Current Drifter Data.

winds extend northward and the NECC begins to flow to the east past the southern side of the dome. The dome is clearly separated from the coast in June. It is relatively small and near the coast; the thermocline ridge to the west of 90°W is only beginning to shoal at this time.

The countercurrent thermocline ridge shoals from July through October. The dome expands as the thermocline shoals, primarily to the west along the ridge. The east–west dimension of the dome increases from 300 km in June to 1000 km in November. This lengthening seems to coincide more with the band of cyclonic wind stress curl associated with the ITCZ (Fig. 6) than with the band of positive surface current divergence (Fig. 7). Surface current convergence appears over parts of the dome in some months, but this may reflect deficiencies of the ship drift data for estimating surface current divergence. The SE trade winds and NECC remain strong on the southern side of the dome and ridge into November.

The Tehuantepec wind jet begins to blow in November as the ITCZ moves to the south. Shoaling of the thermocline on the north side of the dome at the southern extreme of this jet appears to be forced by cyclonic wind stress curl on the equatorward side of the jet. The dome deepens during December and January as the band of cyclonic curl moves south of the thermocline ridge and the NE trade winds blow strongly over the dome.

Monthly climatologies of SeaWiFS chlorophyll concentration and doming show winter–spring blooms near the coast at the Gulfs of Tehuantepec, Papagayo and Panama (Fig. 8). At the Gulf of Papagayo, this bloom is more closely associated with the wind jet itself than with the thermocline shoaling on the equatorward side of the wind jet. When the Papagayo winds have abated in May, the coastal blooming ends. From May through September, chlorophyll increases offshore along the shoaling thermocline ridge, with a local maximum corresponding very closely to the Costa Rica Dome. Coastal blooming begins again in October at Tehuantepec and December at Papagayo and Panama, when the wind jets initiate mixing of surface waters near the coast.

4. Discussion

A clear annual cycle of the Costa Rica Dome is seen in the monthly climatologies of thermocline

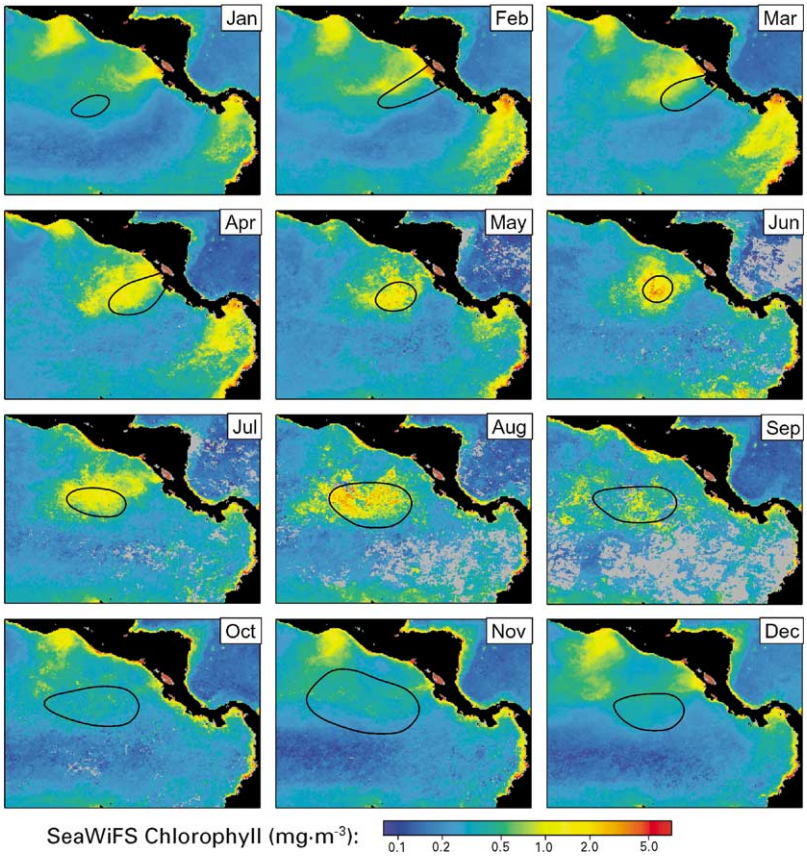

Fig. 8. Monthly mean fields of SeaWiFS chlorophyll concentration in the region of the Costa Rica Dome. Each monthly mean is the mean of three or four Level 3 monthly Standard Mapped Image products (reprocessing #3) from September 1997 to July 2001. SeaWiFS data produced by NASA SeaWiFS Project and distributed by the Distributed Active Archive Center at NASA/Goddard Space Flight Center. Monthly positions of the Costa Rica Dome (35 m thermocline depth contour, thick lines) from Fig. 5.

depth (Fig. 5). The dome may be "permanent" in the sense that thermocline doming and associated cyclonic circulation are always present within the region. However, the dome's location and magnitude (the height and breadth of the dome atop the thermocline ridge) vary considerably during the year. Doming begins near the coast at the Gulf of Papagayo in February–March, moves offshore (WSW) during April–July, intensifies from July through November, then diminishes in December–January. The annual cycles of winds and currents presented here suggest that the observed cycle of doming is closely related to the variability of winds. However, doming and surface circulation are also related.

It is well known that surface currents flow cyclonically around the Costa Rica Dome, and all tropical thermocline domes, as must occur in geostrophic balance. For northern hemisphere domes (Costa Rica, Guinea, Mindanao), this circulation consists of the NECC on the south side, the NEC on the north side, a coastal current between the dome and the coast, and some return flow on the opposite side of the dome. The Costa Rica and Guinea Domes are at the shallow, eastern end of the thermocline ridges between the NEC and NECC in the Pacific and Atlantic; the Mindanao Dome is at the western end of the Pacific countercurrent thermocline ridge, where the thermocline is much deeper at ~ 140 m (Kessler, 1990).

4.1. Winds

The observed stages in the annual cycle of the Costa Rica Dome are closely related to migration of the ITCZ and associated wind stress curl patterns. Local Ekman pumping is consistent with the February–April shoaling of the thermocline at the coast (Fig. 6). Hofmann et al. (1981) noted a correspondence between the mean summer position of the dome and the large-scale wind stress curl field. However, for much of the annual cycle (after the February–April coastal shoaling) in the finer-scale monthly fields presented here, the spatial maximum in the band of positive (cyclonic) wind stress curl associated with the ITCZ is located to the east of the dome. This point has been made previously by Barberán et al. (1986) and Umatani and Yamagata (1991). Spatial mismatches between thermocline domes and positive wind stress curl maxima are also apparent at the Guinea Dome (Bakun, 1987; Siedler et al., 1992) and Mindanao Dome (Harrison, 1989). Accordingly, these authors relate doming to large-scale wind patterns.

The Costa Rica, Guinea, and Mindanao Domes all exhibit seasonal variability that appears to be related to the large-scale wind field, in particular, the convergence of the trade winds in the ITCZ and the associated cyclonic wind stress curl. The Guinea Dome, like the Costa Rica Dome, is more shallow in summer-fall, when the ITCZ lies over the dome and local winds are weak, than in winter, when the ITCZ is south of the dome and strong NE trade winds blow over the dome (Siedler et al., 1992). In a similar manner, the Mindanao Dome is more shallow in winter (December–March), when the NE Asian winter monsoon to the north converges into the ITCZ over the dome, than in summer when weaker winds converge to the north of the dome (Masumoto and Yamagata, 1991). Although all tropical domes seem to be related in some way to the large-scale wind field, the winter Papagayo wind jet is a small-scale feature of the wind field that is unique to the Costa Rica Dome.

The observations summarized and analyzed here show that doming is initiated near the coast in February on the equatorward side of the Papagayo wind jet. Ekman pumping velocities calculated from wind stress curl according to the algorithm of Xie and Hsieh (1995) can reach values as high as $0.5\,\mathrm{m\,d^{-1}}$ at this location (Fig. 9, only February and August are presented here because the spatial patterns are very similar to the wind stress curl patterns in Fig. 6). Wyrtki (1964) estimated an average upwelling velocity of $\sim 0.1\,\mathrm{m\,d^{-1}}$ from the steady-state heat balance of the Costa Rica Dome. The dome deepens in December when the NE trade winds begin to blow strongly and the thermocline is eroded by wind mixing. Mean monthly temperature profiles (Fig. 10) illustrate that the surface layer over the dome becomes mixed and the thermocline becomes both deeper and weaker between November and February.

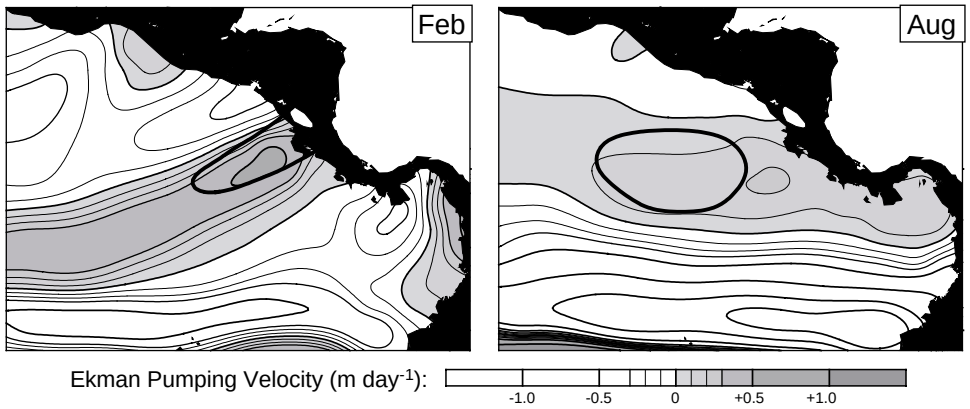

Fig. 9. February and August monthly mean fields of Ekman pumping velocity in the region of the Costa Rica Dome, calculated from wind stress curl (Xie and Hsieh, 1995). Monthly positions of the Costa Rica Dome (35 m thermocline depth contour, thick lines) from Fig. 5.

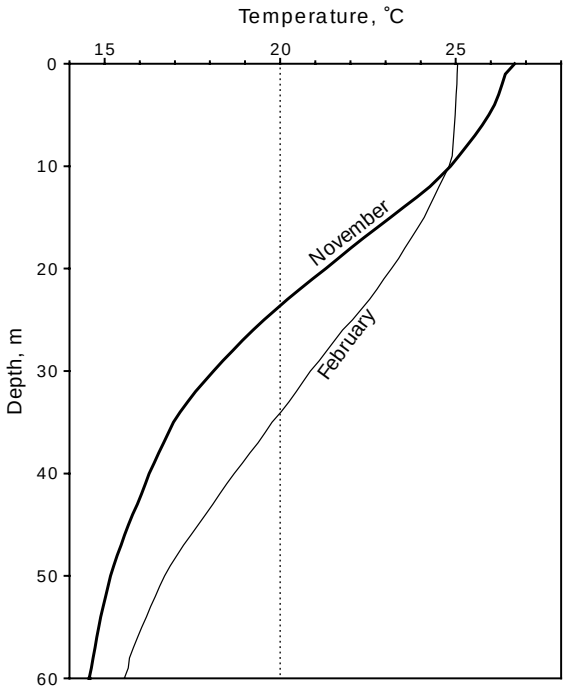

Fig. 10. Monthly mean temperature profiles near the center of the Costa Rica Dome (8–10°N, 89–91°W). Data from World Ocean Database 1998 (Conkright et al., 1999). $N = 183$ (November), $N = 85$ (February).

In contrast to the effects of local winds apparent in the results presented above, remote forcing by winds has been shown to cause seasonal changes in doming in a series of model studies of the three tropical thermal domes. Coastal downwelling Kelvin waves weaken the Guinea Dome in November–December and April–July (Yamagata and Iizuka, 1995). Downwelling long Rossby waves initiate decay of the Mindanao Dome in March–April (Masumoto and Yamagata, 1991). As described above, model coastal eddies weaken the Costa Rica Dome in December–January and then initiate regeneration of the dome in February–March (Umatani and Yamagata, 1991).

4.2. Coastal eddies

Both anticyclonic and cyclonic eddies have been observed propagating from the coast near the Gulf of Papagayo during late fall and winter (Giese et al., 1994; Willett, 1996; Müller-Karger and Fuentes-Yaco, 2000). Willett (1996) conducted a comprehensive study of anticyclonic eddies generated by winter wind jets at the Gulfs of Tehuantepec and Papagayo. In seven years of satellite altimeter data, she detected two to three Papagayo eddies per year generated between October and February. These eddies moved west–southwest, then west, at a mean speed of 11.8 cm s^{-1} for 2–8 months before dissipating west of 100°W in the seasonally strengthening NECC.

The Papagayo and Tehuantepec wind jets also generate cyclonic eddies on the opposite, equatorward side of the jets. These cyclonic eddies are

weaker and shorter lived than the anticyclonic eddies (McCreary et al., 1989), but have been observed in sea surface temperature and ocean color imagery (Stumpf and Legeckis, 1977; Müller-Karger and Fuentes-Yaco, 2000). Müller-Karger and Fuentes-Yaco (2000) observed both anticyclonic and cyclonic "mesoamerican" eddies with translation speeds of 14–16 cm s^{-1}.

The model of Umatani and Yamagata (1991), and the present results, show regeneration of the dome in late winter near the coast. In a model experiment driven by May winds year-round (no winter wind jets), the countercurrent thermocline ridge was formed along 10°N, but not the Costa Rica Dome at the eastern end of the ridge (Fig. 11(b) in Umatani and Yamagata, 1991). Umatani and Yamagata (1991) argued that this experiment demonstrated that a coastal cyclonic eddy is necessary to "seed" the regeneration of the dome.

The *coastal shoaling* and *separation from the coast* stages in the seasonal evolution of the dome (Fig. 5) may reflect, at least in part, the generation and offshore movement of cyclonic coastal eddies. At a nominal speed of 12 cm s^{-1}, a cyclonic eddy would move 310 km in one month, approximately equal to the distance between minima in the thermocline depth climatologies at the coast in February and offshore in March. However, the role of cyclonic coastal eddies in the late winter to spring evolution of the Costa Rica Dome cannot be resolved in the monthly climatologies presented here.

This study has addressed the annual cycle of doming and the factors that influence seasonal variability of the Costa Rica Dome. The data and analysis used here were not appropriate for examining interannual variability. However, the National Center for Environmental Prediction's Ocean Data Assimilation System uses a dynamic ocean model to assimilate sparse temperature data and produce subsurface temperature fields from which thermocline depth can be calculated (Behringer et al., 1998). The results for months of July

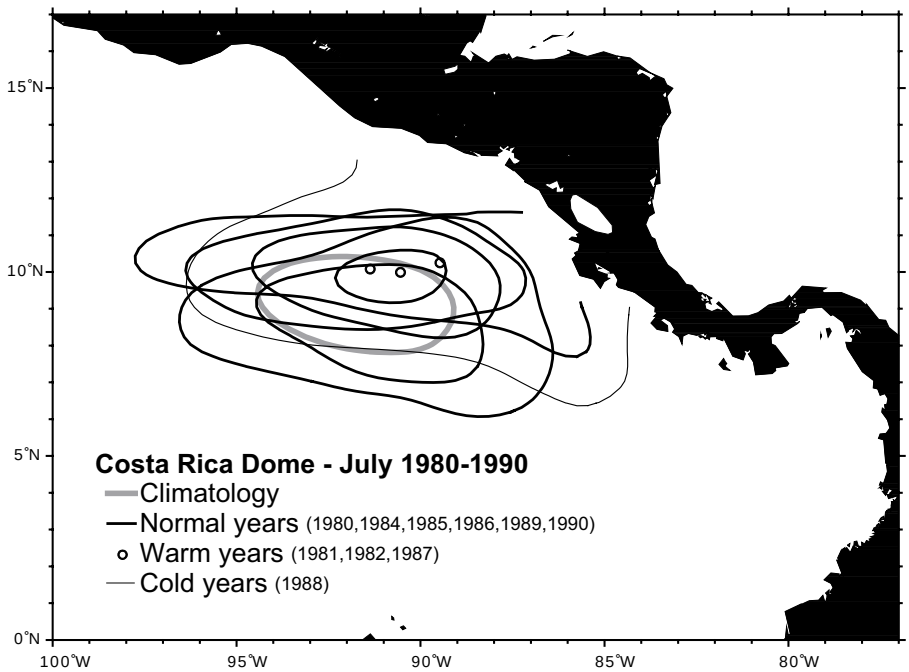

Fig. 11. July 1980–1990 positions of the Costa Rica Dome (35 m thermocline depth contour). For the warm years of 1981, 1982, and 1987, ○ marks the peak of a thermocline dome deeper than 35 m (no dome was evident in 1983). Data from National Center for Environmental Prediction's Ocean Data Assimilation System (Behringer et al., 1998).

from 1980 to 1990 show that the location and magnitude of the Costa Rica Dome can vary almost as much between years as within a year (Fig. 11).

4.3. Biological effects of the dome

Biological sampling of the Costa Rica Dome region has not been adequate for resolving monthly climatologies, with the exception of satellite ocean color data (Fig. 8). The SeaWiFS climatologies show patterns that can be related to variability in thermocline depth and associated processes implied by the physical data. A regional maximum in chlorophyll concentration is present in surface waters over the dome from May to September. The association between high chlorophyll and the thermocline dome is very close during these months.

High chlorophyll levels off the Gulf of Tehuantepec in October–March and Gulf of Papagayo in December–April could be due to nutrient enrichment of the surface layer by wind mixing and/or Ekman pumping associated with the winter wind jets (Trasviña et al., 1995). Winter winds at the Gulf of Papagayo lag those at the Gulf of Tehuantepec by one to two months (monthly mean winds exceed $3\,m\,s^{-1}$ from October to February at the Gulf of Tehuantepec and from December to April at the Gulf of Papagayo). The high winter productivity associated with both the Papagayo and Tehuantepec wind jets is centered directly beneath the jets, indicating the importance of wind mixing. In contrast, doming occurs on the equatorward side of the Papagayo jet where wind stress curl is positive, reflecting the importance of Ekman pumping or upwelling in this process.

High primary productivity at the Costa Rica Dome, and along the thermocline ridge to the west of the dome, is supported by nutrients brought to the surface by wind mixing and/or upwelling (Broenkow, 1965; King, 1986). The thermocline in the eastern tropical Pacific is relatively strong and permanent: there is no deep winter mixing to

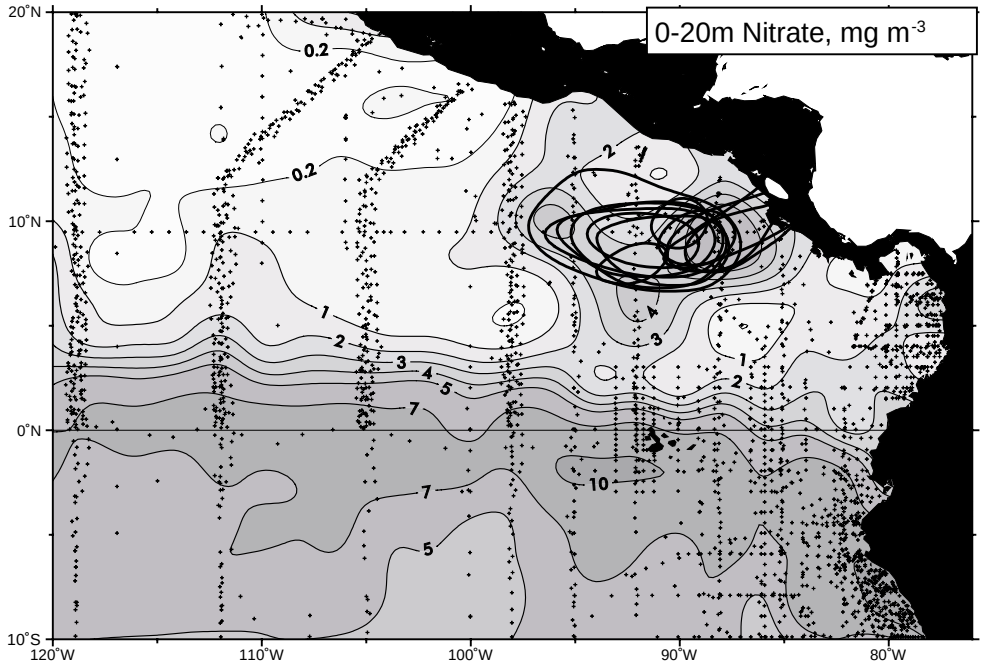

Fig. 12. Mean 0–20 m nitrate concentration in the region of the Costa Rica Dome. Data from 1960–1989 profiles in the on-line NODC Oceanographic Profile Data Base ($n = 1276$). Monthly positions of the Costa Rica Dome (35 m thermocline depth contour, thick lines) from Fig. 5.

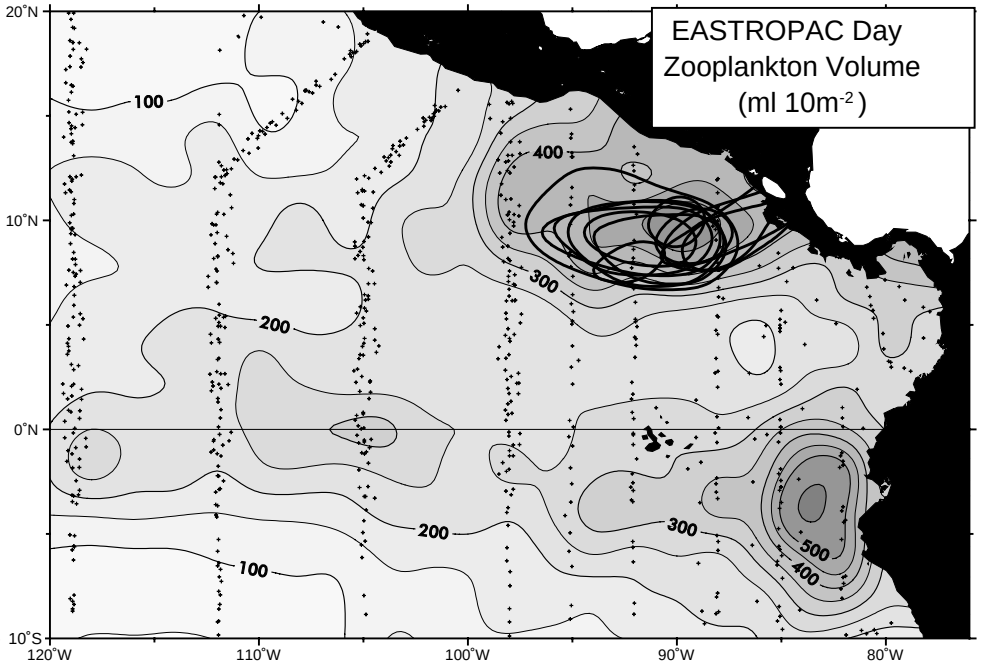

Fig. 13. Mean daytime zooplankton volume from 333 μm mesh nets on EASTROPAC surveys, 1967–1968. Monthly positions of the Costa Rica Dome (35 m thermocline depth contour, thick lines) from Fig. 5.

inject nutrients into the surface layer. Shoaling of the thermocline puts cold, nutrient-rich water close to the surface. Since turbulent motions driven by wind stress on the sea surface decrease exponentially below the surface, shoaling of the thermocline can have a large effect on the input of nutrients into the surface layer. The nitrate climatology (Fig. 12) shows that the surface layer in the region of the dome is enriched (see Peña et al. (1994) for a surface nitrate climatology of the entire tropical Pacific).

Nitrate is the limiting nutrient in tropical Pacific waters where iron is adequate for nutrient uptake (Barber and Chavez, 1991). Iron availability is not as low at the Costa Rica Dome as it is in the high-nitrate low-chlorophyll regions of the equatorial and subarctic Pacific and Southern Ocean (Fung et al., 2000). Mixing and upwelling of waters near the coast by the Papagayo wind jet could be a source of iron. Recent research may elucidate the role of iron and other factors in the productivity of the Costa Rica Dome (Bruland, K. pers. comm., University of California Santa Cruz).

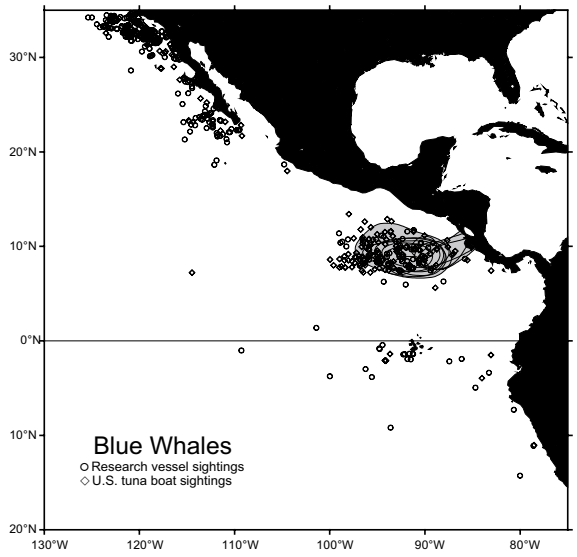

Fig. 14. Sighting locations of blue whales (*Balaenoptera musculus*) from research vessels (1976–1999, $n = 327$) and US tuna boats (1971–1990, $n = 191$) in the NOAA/NMFS/SWFSC sightings database. Monthly positions of the Costa Rica Dome (35 m thermocline depth contour, thin lines) from Fig. 5.

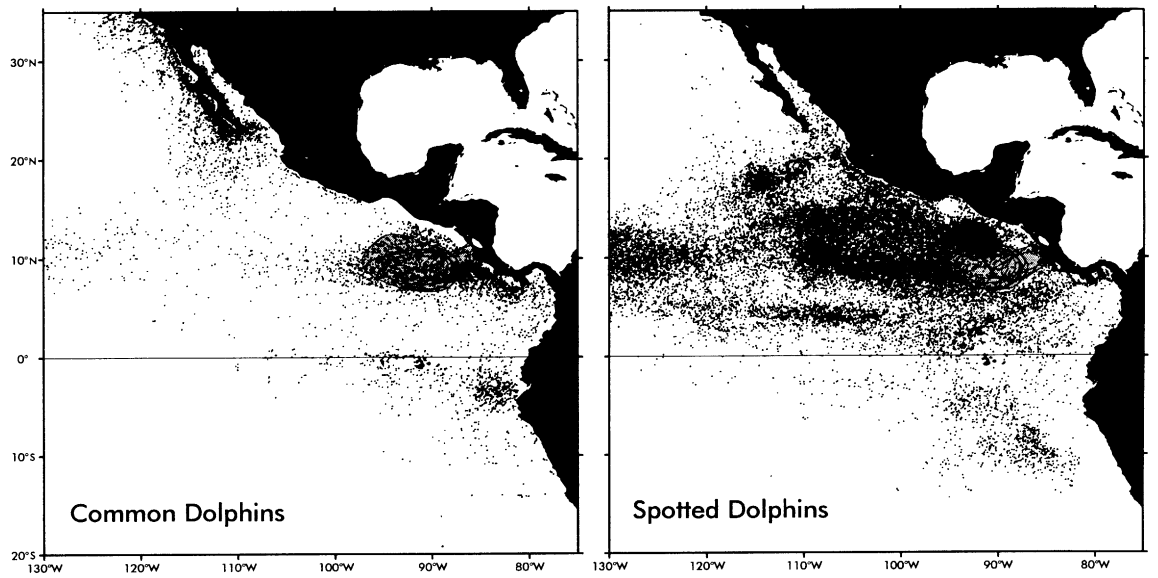

Fig. 15. Sighting locations of common dolphins (*Delphinus delphis*) and spotted dolphins (*Stenella attenuata*) from research and tuna vessels in the NOAA/NMFS/SWFSC sightings database (1971–1999). Monthly positions of the Costa Rica Dome (35 m thermocline depth contour, thin lines) from Fig. 5.

Zooplankton data from the 1967 to 1968 EASTROPAC program show that the high primary production in the region of the Costa Rica Dome supports a high zooplankton biomass (Fig. 13). Mean biomass there is as high or higher than in the equatorial upwelling zone. Larger animals at higher trophic levels are also affected by the dome. Blue whales observed year-round at or near the dome (Fig. 14) may be feeding on large standing stocks of euphausiids (Reilly and Thayer, 1990). Common dolphins feed on small pelagic fish and squid in upwelling-modified waters off Baja California, along the equator, and both at and east of the Costa Rica Dome (Fig. 15). In contrast, spotted dolphins are relatively rare at the dome. Spotted dolphins feed on fish and squid in the warmest waters of the eastern tropical Pacific, where the thermocline is very strong and slightly deeper than at the dome (Fiedler, 1992). They have evolved a complex feeding association with yellowfin tuna and birds and apparently depend on the tuna to drive prey from the thermocline up to the surface. Perhaps, this association does not function or provides no advantage at the dome where the thermocline is shallower and weaker than to the west.

This study has improved the description of the annual cycle of the Costa Rica Dome, clarified the wind forcing of this cycle, and demonstrated pervasive biological effects of the dome. Further study is needed on the influence of coastal eddies on primary production at the dome, the seasonality of secondary production and the exploitation of this production by predators.

Acknowledgements

I thank the hundreds of scientists and technicians whose observations over the years have made this study possible. David Behringer, Russ Davis, and Billy Kessler provided helpful comments, but bear no responsibility for remaining shortcomings. Several anonymous reviewers have prompted substantial improvements. Linda Stathoplos of NODC provided the EASTROPAC zooplankton data and Al Jackson of SWFSC provided the marine mammal sightings data. SeaWiFS data

were produced by the SeaWiFS Project (Code 970.2) and distributed by the Distributed Active Archive Center (Code 902) at the Goddard Space Flight Center, Greenbelt, MD 20771, sponsored by NASA's Mission to Planet Earth Program. Finally, I thank Steve Reilly of SWFSC for continued support of marine mammal habitat studies.

References

Arnault, S., 1987. Tropical Atlantic geostrophic currents and ship drifts. Journal of Geophysical Research 92, 5076–5088.

Bakun, A., 1987. Applications of maritime data to the study of surface forcing of seasonal and interannual ocean variability in eastern boundary regions. Ph.D. Thesis, Oregon State University, 226pp.

Barber, R.T., Chavez, F.P., 1991. Regulation of primary productivity rate in the equatorial Pacific. Limnology and Oceanography 36, 1803–1815.

Barberán, J.M., Gallegos, A., Fernández, A., Mee, L.D., 1986. Subsurface origin of the Costa Rica Dome, unpublished.

Behringer, D.W., Ji, M., Leetmaa, A., 1998. An improved coupled model for ENSO prediction and implications for ocean initialization. Part I: the ocean data assimilation system. Monthly Weather Review 126, 1013–1021.

Broenkow, W.W., 1965. The distribution of nutrients in the Costa Rica Dome in the eastern tropical Pacific Ocean. Limnology and Oceanography 10, 40–52.

Chelton, D.B., Freilich, M.H., Esbensen, S.K., 2000a. Satellite observations of the wind jets off the Pacific coast of Central America. Part I: case studies and statistical characteristics. Monthly Weather Review 128, 1993–2018.

Chelton, D.B., Freilich, M.H., Esbensen, S.K., 2000b. Satellite observations of the wind jets off the Pacific coast of Central America. Part II: regional relationships and dynamical considerations. Monthly Weather Review 128, 2019–2043.

Conkright, M.E., Levitus, S., O'Brien, T., Boyer, T.P., Stephens, C., Johnson, D., Baranova, O., Antonov, J., Gelfeld, R., Rochester, J., Forgy, C., 1999. World ocean database 1998 CD-ROM data set documentation, Version 2.0. NODC Internal Report 14, 116pp.

Cromwell, T., 1958. Thermocline topography, horizontal currents and "ridging" in the eastern tropical Pacific. Bulletin Inter-American Tropical Tuna Commission 111, 135–164.

da Silva, A.M., Young, C.C., Levitus, S., 1994. Atlas of surface marine data 1994. Algorithms and Procedures, Vol. 1. NOAA Atlas NESDIS 6, US Government Printing Office, Washington D.C. 83pp.

Fiedler, P.C., 1992. Seasonal climatologies and variability of eastern tropical Pacific surface waters. NOAA Technical Report NMFS 109, 65pp.

Fung, I.Y., Meyn, S.K., Tegen, I., Doney, S.C., John, J.G., Bishop, J.K.B., 2000. Iron supply and demand in the upper ocean. Global Biogeochemical Cycles 14, 281–295.

Giese, B.S., Carton, J.A., Holl, L.J., 1994. Sea level variability in the eastern tropical Pacific as observed by TOPEX and tropical ocean-global atmosphere tropical atmosphere-ocean experiment. Journal of Geophysical Research 99, 24739–24748.

Harrison, D.E., 1989. On climatological monthly mean wind stress and wind stress curl fields over the world ocean. Journal of Climate 2, 57–70.

Hofmann, E.E., Busalacchi, A.J., O'Brien, J.J., 1981. Wind generation of the Costa Rica Dome. Science 214, 552–554.

Kessler, W.S., 1990. Observations of long Rossby waves in the northern tropical Pacific. Journal of Geophysical Research 95, 5183–5217.

King, F.D., 1986. The dependence of primary production in the mixed layer of the eastern tropical Pacific on the vertical transport of nitrate. Deep-Sea Research I 33, 733–754.

Large, W.G., Pond, S., 1981. Open ocean momentum flux measurements in moderate to strong winds. Journal of Physical Oceanography 11, 324–336.

Masumoto, Y., Yamagata, T., 1991. Response of the western tropical Pacific to the Asian winter monsoon: the generation of the Mindanao Dome. Journal of Physical Oceanography 21, 1386–1398.

Mazeika, P.A., 1967. Thermal domes in the eastern tropical Atlantic Ocean. Limnology and Oceanography 12, 537–539.

McCreary, J.P., Lee, H.S., Enfield, D.B., 1989. The response of the coastal ocean to strong offshore winds: with application to circulations in the Gulfs of Tehuantepec and Papagayo. Journal of Marine Research 47, 81–109.

Müller-Karger, F.E., Fuentes-Yaco, C., 2000. Characteristics of wind-generated rings in the eastern tropical Pacific Ocean. Journal of Geophysical Research 105, 1271–1284.

Peña, M.A., Lewis, M.R., Cullen, J.J., 1994. New production in the warm waters of the tropical Pacific Ocean. Journal of Geophysical Research 99, 14255–14268.

Reilly, S.B., Thayer, V.G., 1990. Blue whale (*Balaenoptera musculus*) distribution in the eastern tropical Pacific. Marine Mammal Science 6, 265–277.

Richardson, P.L., 1997. Drifting in the wind: Leeway error in shipdrift data. Deep-Sea Research I 44, 1877–1903.

Roy, C., Mendelssohn, R., 1995. CODE (Comprehensive Ocean Dataset Extraction). User's Guide. NOAA/NMFS/Pacific Fisheries Environmental Group, Monterey, CA.

Siedler, G., Zangenberg, N., Onken, R., 1992. Seasonal changes in the tropical Atlantic circulation: observation and simulation of the Guinea Dome. Journal of Geophysical Research 97, 703–715.

Stumpf, H.G., Legeckis, R.V., 1977. Satellite observations of mesoscale eddy dynamics in the eastern tropical Pacific Ocean. Journal of Physical Oceanography 7, 648–658.

Trasviña, A., Barton, E.D., Brown, J., Velez, H.S., Kosro, P.M., Smith, R.L., 1995. Offshore wind forcing in the Gulf of Tehuantepec, Mexico: the asymmetric circulation. Journal of Geophysical Research 100, 20649–20663.

Umatani, S., Yamagata, T., 1991. Response of the eastern tropical Pacific to meridional migration of the ITCZ: the generation of the Costa Rica Dome. Journal of Physical Oceanography 21, 346–363.

Voituriez, B., 1981. Northern and southern equatorial undercurrents and the formation of tropical thermal domes. Oceanologica Acta 4, 497–506.

Willett, C.S., 1996. A study of anticyclonic eddies in the eastern tropical Pacific Ocean with integrated satellite, in situ, and modeled data. Ph.D. Thesis, University of Colorado, 127pp.

Wyrtki, K., 1961. Physical oceanography of the southeast Asian waters. Naga Reports 2, 195pp.

Wyrtki, K., 1964. Upwelling in the Costa Rica Dome. Fishery Bulletin 63, 355–372.

Xie, L., Hsieh, W., 1995. The global distribution of wind-induced upwelling. Fisheries Oceanography 4, 52–67.

Yamagata, T., Iizuka, S., 1995. Simulation of the tropical thermal domes in the Atlantic: a seasonal cycle. Journal of Physical Oceanography 25, 2129–2140.